

Tunneling Spectroscopy at Megabar Pressures: Determination of the Superconducting Gap in Sulfur

F. Du,^{1,*} F. F. Balakirev², V. S. Minkov,¹ G. A. Smith², B. Maiorov², P. P. Kong,¹
A. P. Drozdov,¹ and M. I. Erements^{1,†}

¹Max Planck Institute for Chemistry, Hahn Meiter Weg 1, Mainz 55128, Germany

²National High Magnetic Field Laboratory, Los Alamos National Laboratory,
Los Alamos, New Mexico 87545, USA



(Received 22 February 2024; accepted 31 May 2024; published 17 July 2024)

The recent discovery of high-temperature, high-pressure superconductors, such as hydrides and nickelates, has opened exciting avenues in studying high-temperature superconductivity. The primary superconducting properties of these materials are well characterized by measuring various electrical and magnetic properties, despite the challenges posed by the high-pressure environment. Experimental microscopic insight into the pairing mechanism of these superconductors is even more challenging, due to the lack of direct probes of the superconducting gap structures at high pressure conditions. Here, we have developed a planar tunnel junction technique for diamond anvil cells and present ground-breaking tunneling spectroscopy measurements at megabar pressures. We determined the superconducting gap of elemental sulfur at 160 GPa, a key constituent of the high-temperature superconductor H₃S. High quality tunneling spectra indicate that β -Po phase sulfur is a type II superconductor with a single *s*-wave gap with a gap value $2\Delta(0) = 5.6$ meV. This technique is compatible with superconducting compounds synthesized in diamond anvil cells and provides insight into the pairing mechanism in novel superconductors under high-pressure conditions.

DOI: [10.1103/PhysRevLett.133.036002](https://doi.org/10.1103/PhysRevLett.133.036002)

High pressures have enabled the realization of desired chemical compositions and physical properties in materials that do not exist at ambient conditions, where near-room temperature superconductivity in hydrogen-rich compounds [1–3] and high-temperature superconductivity in nickelates [4] are two striking examples of many exciting discoveries. The superconducting pairing in these materials induces an energy gap in the quasiparticle density near the Fermi energy. The size and symmetry of the superconducting gap are fundamentally related to the nature of the superconducting coupling mechanism, but the experimental determination of the superconducting gap in a high-pressure environment is quite challenging.

Tunneling spectroscopy is a direct probe of the electronic density of states, and thus, allows for examination of the structure of the electronic excitation spectrum near the Fermi energy [5]. The formation of the superconducting band gap predicted by the Bardeen-Cooper-Schrieffer (BCS) theory in conventional superconductors was

validated by tunneling spectroscopy [5,6]. Tunneling spectroscopy also captured pseudogap and nodal gap features in non-BCS high-temperature cuprate superconductors [7].

The tunneling spectroscopy has been developed so far with pressure up to 3 GPa in piston or Bridgman pressure cells [8–10] where planar tunnel junctions were fabricated before loading into the pressure cell. The extreme pressure environment affects the properties and integrity of the tunneling barrier, leading to leakage currents and a reduction in the magnitude of the potential energy barrier. This challenging technique is difficult to apply to diamond anvil cell (DAC) with a micrometer size sample. The most interesting materials, such as hydrogen-rich high-temperature superconductors, can only be synthesized at high pressures, rendering preformed junctions unusable in such cases.

We have developed an *in situ* method for fabricating planar tunnel junctions in diamond anvil cell environments, enabling us to extend tunneling spectroscopy measurements to pressures beyond the megabar range. Employing this technique, we investigated the superconducting properties of elemental sulfur. Sulfur, an insulating molecular solid at ambient pressure, undergoes an insulator-to-metal transition and becomes superconducting above 90 GPa [11–14]. Here we have pressurized sulfur to 160 GPa, where a superconducting transition temperature T_c of 17 K was reported in the rhombohedral lattice [13,15,16].

Published by the American Physical Society under the terms of the [Creative Commons Attribution 4.0 International license](https://creativecommons.org/licenses/by/4.0/). Further distribution of this work must maintain attribution to the author(s) and the published article's title, journal citation, and DOI. Open access publication funded by the Max Planck Society.

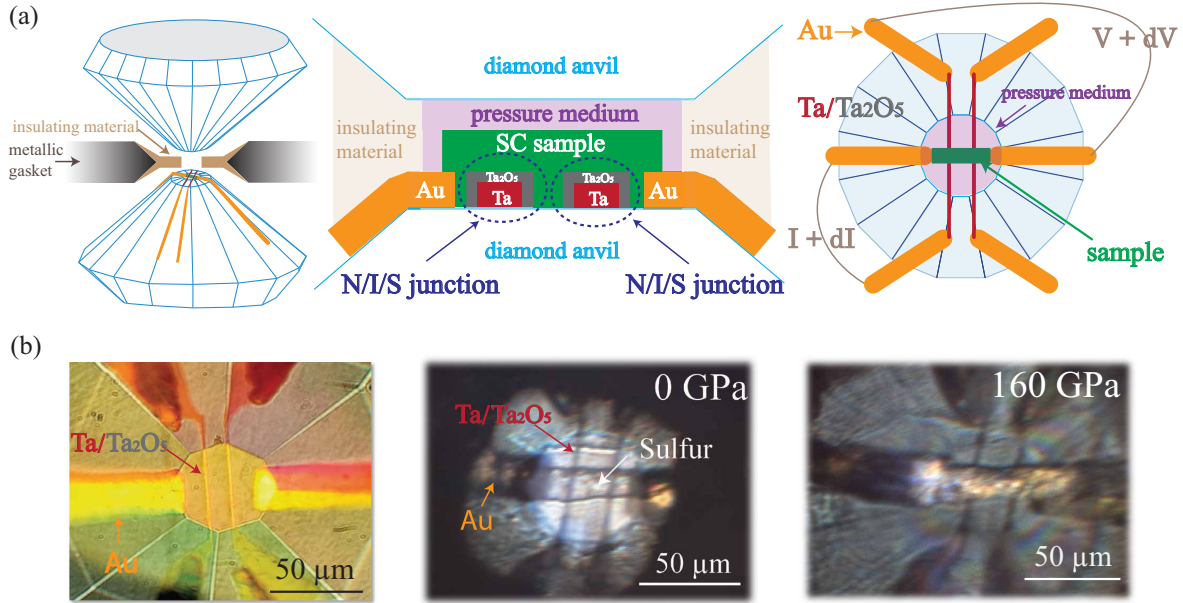


FIG. 1. Fabrication of planar tunneling junctions. (a) Schematic of planar tunneling junction fabrication between two opposing anvils. Electrical leads are deposited on the bottom anvil. A rectangular sample (green) is loaded above the electric leads. The insulating material is used to isolate electrical leads from the metallic gasket. Detailed views of the region between the two opposing anvil tips after pressurization are shown from side and top perspectives. Gold traces are marked as thick gold lines, while tantalum traces with Ta oxidize layer are colored as wine and gray area, respectively. Sulfur sample is marked as green area which is surrounded by pressure medium (marked as light purple area). The Ta/Ta₂O₅/sulfur junction areas are indicated by blue dashed oval. See Fig. S1 [21] for more details on the fabrication of the junctions and description of the differential conductance measurements. (b) Optical microscope images through the top diamond anvil before sample loading and after sample loading at ambient pressure, and at 160 GPa. Sulfur piece is transparent at ambient pressure and shows metallic luster at 160 GPa. Scale bars of 50 μm are shown for reference.

Distinct superconducting gap features have been observed in tunneling spectra below T_c . Temperature and magnetic field dependence of tunneling spectra have been analyzed with the Blonder-Tinkham-Klapwijk (BTK) model [17], from which we deduce the gap value of $2\Delta(0) = 5.6$ meV and reveal a single s -wave gap symmetry of the superconducting sulfur.

A planar tunnel junction comprises three essential components: normal metal (N), insulating barrier (I), and superconducting sample (S). In our study, the critical aspect lies in the preparation of the metal and barrier components on the anvil tip. Tantalum (Ta) and its oxides were chosen to serve as the $N - I$ components of the junction. Tantalum pentoxide (Ta₂O₅), selected as the insulating barrier, offers notable advantages due to its high stability and density, making it a superior choice for tunneling junctions [18,19]. In comparison to other common barrier materials like Al₂O₃ and MgO, Ta₂O₅ requires a greater thickness to achieve the same barrier height. This characteristic results in the current distribution in the barrier being less sensitive to fluctuations in thickness [20], rendering it an excellent candidate for the insulating barrier material in high-pressure tunneling devices.

The tunnel junction preparation process was schematically illustrated in Fig. 1(a) and Fig. S1 [21]. Initially, six gold traces were deposited on the diamond anvils, followed

by the deposition of two tantalum leads with thickness of ~ 15 nm and a few micrometers wide on the anvil tip, connected to the outer gold traces. Notably, the resistivity of Ta film at 160 GPa has been measured down to 2 K, above which no superconducting transition is observed (Fig. S2 [21]). Subsequently, a tantalum oxide layer was grown on the surface of Ta through the oxidization procedure [21]. A rectangular polycrystalline sulfur piece was then placed on the prepared probes. After pressurizing the sulfur piece, two NIS junctions were fabricated, located at the cross area on the anvil tip, marked by the blue dashed oval in Fig. 1(a). The molecular sulfur has been characterized using Raman spectroscopy at ambient pressure [Fig. S3(a) [21]], which is consistent with the previous work [27]. Upon pressurising, sulfur transforms from a transparent insulator to an opaque metal, as seen in Fig. 1(b). X-ray diffraction measurements indicated that sulfur, pressurized to 160 GPa, adopts the β -Po crystal lattice [Fig. S3(b) [21]], for which T_c of ~ 17 K was reported [13,15].

To detect and characterize the superconducting gap features of sulfur, we conducted differential conductance measurements as a function of temperature across the junctions. Figure 2(a) illustrates the original data for junction 1 (The data for junction 2 is shown in Fig. S4 [21]). In the nonsuperconducting state above T_c , the tunnel

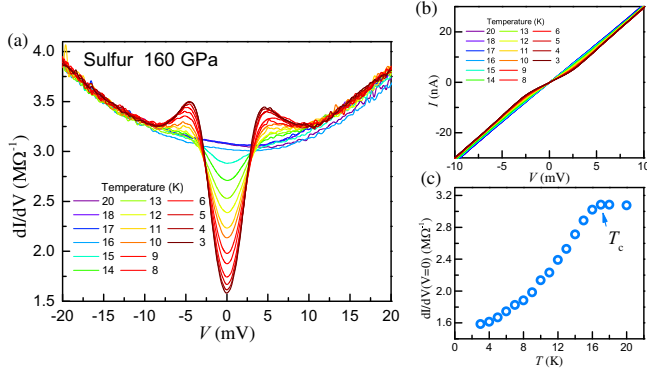


FIG. 2. Temperature evolution of tunneling spectra. (a) Tunneling spectra for junction 1 at several temperatures below 20 K. Differential conductance is plotted as a function of applied voltage. (b) Temperature variation of current-voltage characteristics corresponding to (a). (c) Temperature evolution of differential conductance at zero bias voltage. The arrow indicates the superconducting transition.

junction resistance was of the order of 100 k Ω , with a junction area of $\sim 60 \mu\text{m}^2$, indicating a good quality of insulating barrier. At the lowest measured temperatures, quasiparticle peaks emerge in the tunneling spectra at positions of $\pm\Delta_p \approx \pm 4.5 \text{ meV}$, which stem from the appearance of the superconducting gap. The differential conductance between two quasi-particle peaks shows pronounced suppression, as quasiparticle states with energy below the gap are forbidden in the superconducting phase. As the temperature increases, quasiparticle peaks broaden, and the distance between the peaks decreases as the magnitude of the superconducting gap diminishes. Notably, the differential conductance in the normal state exhibits an asymmetric parabolic behavior (Fig. S5 [21]), which is attributed to a slight asymmetry in the potential barrier shape [28]. The T_c of approximately 17 K can be estimated from the temperature evolution of zero bias differential conductance [Fig. 2(c)], consistent with previous reports [13,15].

In principle, gap values could be determined directly from the distance between the quasiparticle coherence peaks Δ_p . However, gap values might be overestimated at finite temperatures with Δ_p due to the thermal smearing and inelastic scattering effects. To address this, we utilized BTK model [17] to estimate gap values at various temperatures. The BTK model is a general framework for describing transport properties across the interface between the normal metal and a superconductor, with a finite barrier at the interface. The gap value Δ , quasiparticle smearing parameter Γ , and barrier strength Z are adjustable fitting parameters in this model (see details in Supplemental Material [21]). As displayed in Fig. 3(a), the normalized differential conductance at different temperatures fits well with a single-gap s -wave BTK model. We also used a d -wave BTK model to fit the data. However, it does not fit

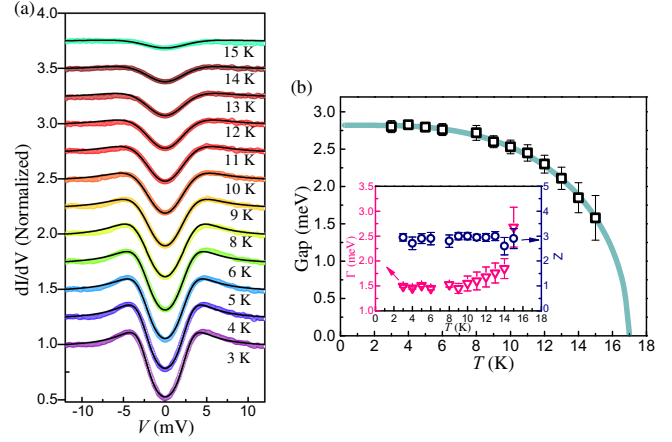


FIG. 3. Tunneling spectra with fits to BTK model at various temperatures. (a) Normalized differential conductance spectra for junction 1 (colored data) together with single s -wave BTK fitting (solid black curves). The tunneling spectra are normalized by dividing differential conductance in superconducting state by the conductance measured in the normal state at 18 K: $G(V)/G_{18K}(V)$. Spectra above 3 K are offset vertically for clarity. (b) Superconducting gap values Δ are obtained from the BTK model fit. The solid green line is the gap value predicted by the BCS model. Inset: quasiparticle smearing parameter Γ and barrier strength Z transition from BTK model. Error bars are from BTK fitting error.

well, as shown in Fig. S6 [21]. The resulting fit parameters of s -wave BTK model are presented in Fig. 3(b). The estimated barrier strength Z is around 3, indicative of proximity to the tunneling limit. The temperature evolution of gap values can be well described with BCS theory (green curve), from which the gap value at zero temperature $2\Delta(0) = 5.6 \text{ meV}$ and $2\Delta(0)/k_B T_c = 3.8$ can be extracted. The moderately higher value of $2\Delta(0)/k_B T_c$ ratio, relative to the BCS value of 3.52, suggests that sulfur is a strongly coupled superconductor.

We also investigated the evolution of the superconducting gap with magnetic field at different temperatures. As displayed in Figs. 4(a)–4(d), superconducting gap is gradually suppressed with increasing magnetic fields, presenting characteristics of a type II superconductor. The spectra are well fitted with the BTK model (solid lines), from which the gap value as a function of magnetic field were extracted as shown in Fig. 4(e). The magnetic field dependence of gap values Δ follow the typical formula $\Delta = \Delta(B=0)\sqrt{1-H/H_c}$ for a fully gapped superconductor, where H_c is the critical field [29]. The $\mu_0 H_{c2}(T)$ could be estimated from the evolution of zero bias conductance under applied magnetic fields. The temperature dependence of $\mu_0 H_{c2}(T)$ is well described by a classical Werthamer-Helfand-Hohenberg (WHH) model [30] as shown in Fig. 4(f), suggesting that orbital limiting is the dominant pair-breaking mechanism in superconducting sulfur. The extrapolated $\mu_0 H_{c2}(0)$ is

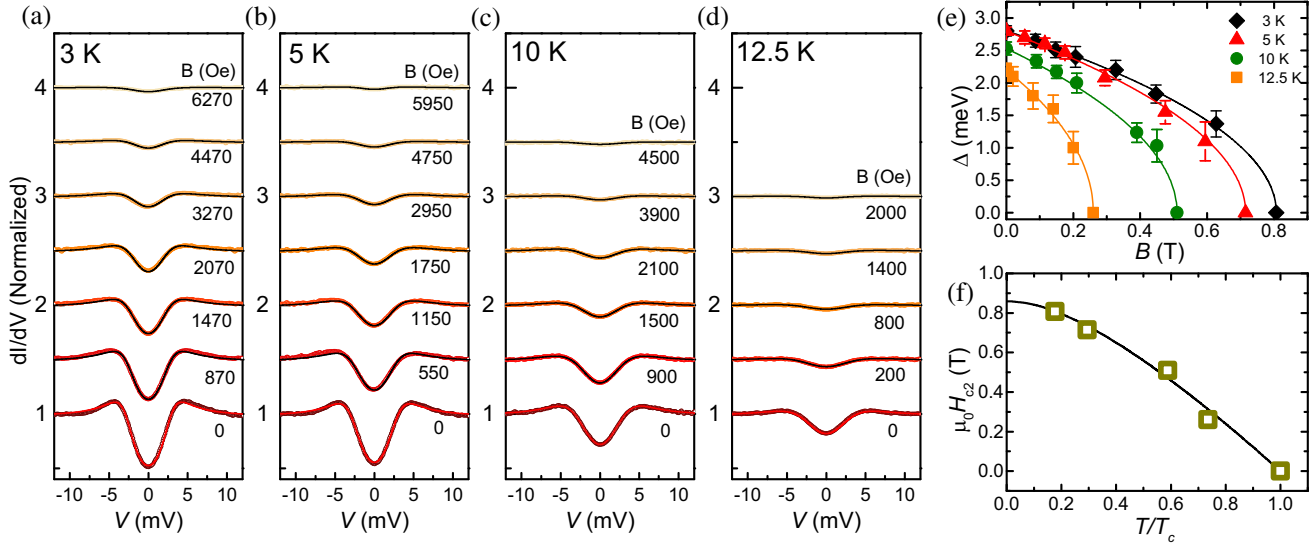


FIG. 4. The effect of an external magnetic field on the tunneling spectra. (a)–(d) Normalized tunneling spectra for junction 1 (colored data) together with the single-band s -wave BTK fits (solid curves) in magnetic field of different magnitude at various temperatures. Spectra above 0 T are shifted for clarity. (e) Magnetic field evolution of fitted gap values Δ at different temperatures from the BTK model (solid symbols), compared with the square root field dependence (solid curves). Error bars are from the BTK fitting error. (f) The upper critical field [extracted from temperature evolution of $G(0)$ in Fig. S7 [21] as a function of temperature]. The solid lines correspond to the WHH fit.

~ 0.86 T, from which the coherence length ξ is estimated as 19.5 nm using Ginzburg-Landau theory.

As one of the highest T_c elemental superconductors, sulfur has attracted considerable research interest. Apart from the experimental identification of T_c by magnetic susceptibility and resistivity measurements [1,13,15], the superconducting properties of sulfur in the rhombohedral β -Po phase have also been investigated theoretically [31–33]. Crucially, our research has validated the accuracy of modern superconducting density functional theory [31] in predicting superconductor properties from first principles. Consistent with our tunneling spectra indicating a single s -wave gap at low temperature, the calculations predict that band anisotropy of the electron-phonon coupling strength λ is weak and there is minimal variation in calculated T_c between “isotropic” and “multiband” approaches [31]. The tunneling spectra under external magnetic fields demonstrate that the critical field is well below the Pauli limit, again suggesting a singlet pairing of Cooper pairs.

The fabrication of tunnel junctions directly on a diamond anvil offers several advantages over traditional methods designed for large volume cells. The $N-I$ part is pre-deposited on the anvil tip, while the S part is synthesized directly in a pressure chamber between the anvils. Notably, the initial state of the precursors is not confined to the solid phase; liquid and gaseous precursors can also be utilized in this approach. These advantages position the technique as promising for a diverse array of superconductors under high-pressure conditions. For instance, the

high-temperature superconductors hydrogen sulphide H_2S and H_3S have been synthesized by pressurising H_2S gas to over 150 GPa [1]. It is of great interest to determine the characteristics of the superconducting gap, which would help in the theoretical design of new hydrides with higher T_c .

The utility of tunneling spectroscopy extends beyond the detection of the superconducting gap. This technique enables the investigation of various gap features and excitation spectra, including charge density wave gaps [34], Kondo hybridization gaps [35,36] and linear energy dispersion of Dirac fermions [37]. As such, this method can potentially study the interplay of different electronic phases in correlated systems under pressure.

In summary, we have developed tunneling spectroscopy measurements within a diamond anvil cell environment through *in situ* fabrication of planar tunnel junctions. Tunneling spectra of superconducting sulfur have been measured at a pressure of 160 GPa. Based on the temperature dependence of the tunneling spectra, we conclude that the β -Po phase of sulfur is a conventional BCS superconductor with a gap value at zero temperature $2\Delta(0) = 5.6$ meV. The evolution of the tunneling spectra under magnetic fields indicates that sulfur is a type II superconductor with a critical field $\mu_0 H_{c2}(0)$ of ~ 0.86 T. Our work pioneers tunneling spectroscopy measurements at pressures above one megabar and opens a clear route to directly detect gaplike excitation spectra of electronic phases at high pressures, such as superconducting gap features in hydrogen-rich superconductors.

M. I. E. is thankful to the Max Planck community for their support, and Professor Dr. U. Pöschl for the constant encouragement. We thank Bin Shen and Philipp Gegenwart for help with the experiment. The National High Magnetic Field Laboratory is supported by the National Science Foundation through NSF/DMR-2128556*, the State of Florida, and the U.S. Department of Energy. Parts of this research were carried out at PETRA-III using P02.2. Beam time allocated for proposal I-20221163.

*feng.du@mpic.de

[†]m.eremets@mpic.de

- [1] A. P. Drozdov, M. I. Eremets, I. A. Troyan, V. Ksenofontov, and S. I. Shylin, *Nature (London)* **525**, 73 (2015).
- [2] A. P. Drozdov, P. P. Kong, V. S. Minkov, S. P. Besedin, M. A. Kuzovnikov, S. Mozaffari, L. Balicas, F. F. Balakirev, D. E. Graf, V. B. Prakapenka, E. Greenberg, D. A. Knyazev, M. Tkacz, and M. I. Eremets, *Nature (London)* **569**, 528 (2019).
- [3] P. Kong, V. S. Minkov, M. A. Kuzovnikov, A. P. Drozdov, S. P. Besedin, S. Mozaffari, L. Balicas, F. F. Balakirev, V. B. Prakapenka, S. Chariton, D. A. Knyazev, E. Greenberg, and M. I. Eremets, *Nat. Commun.* **12**, 5075 (2021).
- [4] H. Sun, M. Huo, X. Hu, J. Li, Z. Liu, Y. Han, L. Tang, Z. Mao, P. Yang, B. Wang, J. Cheng, D.-X. Yao, G.-M. Zhang, and M. Wang, *Nature (London)* **621**, 493 (2023).
- [5] I. Giaever, *Phys. Rev. Lett.* **5**, 147 (1960).
- [6] J. Bardeen, L. N. Cooper, and J. R. Schrieffer, *Phys. Rev.* **106**, 162 (1957).
- [7] O. Fischer, M. Kugler, I. Maggio-Aprile, C. Berthod, and C. Renner, *Rev. Mod. Phys.* **79**, 353 (2007).
- [8] V. M. Svistunov, M. A. Belogolovskii, and O. I. Chernyak, *Sov. Phys. Usp.* **30**, 1 (1987).
- [9] J. P. Franck and W. J. Keeler, *Phys. Rev. Lett.* **20**, 379 (1968).
- [10] J. Zhu, Z.-X. Yang, X.-Y. Hou, T. Guan, Q.-T. Zhang, Y.-Q. Li, X.-F. Han, J. Zhang, C.-H. Li, L. Shan, G.-F. Chen, and C. Ren, *Appl. Phys. Lett.* **106**, 202601 (2015).
- [11] H. Luo, S. Desgreniers, Y. K. Vohra, and A. L. Ruoff, *Phys. Rev. Lett.* **67**, 2998 (1991).
- [12] H. Luo, R. G. Greene, and A. L. Ruoff, *Phys. Rev. Lett.* **71**, 2943 (1993).
- [13] V. V. Struzhkin, R. J. Hemley, H. kwang Mao, and Y. A. Timofeev, *Nature (London)* **390**, 382 (1997).
- [14] S. Kometani, M. I. Eremets, K. Shimizu, M. Kobayashi, and K. Amaya, *J. Phys. Soc. Jpn.* **66**, 2564 (1997).
- [15] E. Gregoryanz, V. V. Struzhkin, R. J. Hemley, M. I. Eremets, H.-k. Mao, and Y. A. Timofeev, *Phys. Rev. B* **65**, 064504 (2002).
- [16] V. S. Minkov, V. Ksenofontov, S. L. Budko, E. F. Talantsev, and M. I. Eremets, *Nat. Phys.* **19**, 1293 (2023).
- [17] G. E. Blonder, M. Tinkham, and T. M. Klapwijk, *Phys. Rev. B* **25**, 4515 (1982).
- [18] M. Sharma, S. X. Wang, and J. H. Nickel, *Phys. Rev. Lett.* **82**, 616 (1999).
- [19] G. Mani, D. Porter, K. Grove, S. Collins, A. Ornberg, and R. Shulfer, *J. Biomed. Mater. Res., Part A* **110**, 1291 (2022).
- [20] P. Rottländer, M. Hehn, O. Lenoble, and A. Schuhl, *Appl. Phys. Lett.* **78**, 3274 (2001).
- [21] See Supplemental Material at <http://link.aps.org/supplemental/10.1103/PhysRevLett.133.036002> for experimental methods, BTK model, detailed procedures of tunnel junction fabrication, resistivity of Ta film at 160 GPa, raman spectrum and x-ray diffraction pattern of sulfur, tunneling spectrum for junction 2, differential conductance spectra at normal state, fitting with d-wave BTK model, original tunneling spectra for junction 1 under external magnetic field, and pressure determination, which includes Refs. [22–26].
- [22] M. I. Eremets, V. S. Minkov, P. P. Kong, A. P. Drozdov, S. Chariton, and V. B. Prakapenka, *Nat. Commun.* **14**, 907 (2023).
- [23] C. Prescher and V. B. Prakapenka, *High Press. Res.* **35**, 223 (2015).
- [24] V. Petricek, M. Dušek, and L. Palatinus, *Z. Kristallogr.—Cryst. Mater.* **229**, 345 (2014).
- [25] A. L. Bail, H. Duroy, and J. Fourquet, *Mater. Res. Bull.* **23**, 447 (1988).
- [26] Y. Tanaka and S. Kashiwaya, *Phys. Rev. Lett.* **74**, 3451 (1995).
- [27] M. S. K. S. Andrikopoulos, F. A. Gorelli, and S. N. Yannopoulos, *High Press. Res.* **33**, 134 (2013).
- [28] W. F. Brinkman, R. C. Dynes, and J. M. Rowell, *J. Appl. Phys.* **41**, 1915 (1970).
- [29] E. H. Brandt, *Phys. Status Solidi (b)* **77**, 105 (1976).
- [30] N. R. Werthamer, E. Helfand, and P. C. Hohenberg, *Phys. Rev.* **147**, 295 (1966).
- [31] M. Monni, F. Bernardini, A. Sanna, G. Profeta, and S. Massidda, *Phys. Rev. B* **95**, 064516 (2017).
- [32] J. Whaley-Baldwin, M. Hutcheon, and C. J. Pickard, *Phys. Rev. B* **103**, 214111 (2021).
- [33] O. Degtyareva, M. V. Magnitskaya, J. Kohanoff, G. Profeta, S. Scandolo, M. Hanfland, M. I. McMahon, and E. Gregoryanz, *Phys. Rev. Lett.* **99**, 155505 (2007).
- [34] C. Wang, B. Giambattista, C. G. Slough, R. V. Coleman, and M. A. Subramanian, *Phys. Rev. B* **42**, 8890 (1990).
- [35] H. Pirie, E. Mascot, C. E. Matt, Y. Liu, P. Chen, M. H. Hamidian, S. Saha, X. Wang, J. Paglione, G. Luke, D. Goldhaber-Gordon, C. F. Hirjibehedin, J. C. S. Davis, D. K. Morr, and J. E. Hoffman, *Science* **379**, 1214 (2023).
- [36] A. Aishwarya, Z. Cai, A. Raghavan, M. Romanelli, X. Wang, X. Li, G. D. Gu, M. Hirsbrunner, T. Hughes, F. Liu, L. Jiao, and V. Madhavan, *Science* **377**, 1218 (2022).
- [37] W. K. Park, L. Sun, A. Noddings, D.-J. Kim, Z. Fisk, and L. H. Greene, *Proc. Natl. Acad. Sci. U.S.A.* **113**, 6599 (2016).